

Supplementary Materials

Slow Relaxation of the Magnetization in Bis-Decorated Chiral Helicene-Based Coordination Complexes of Lanthanides

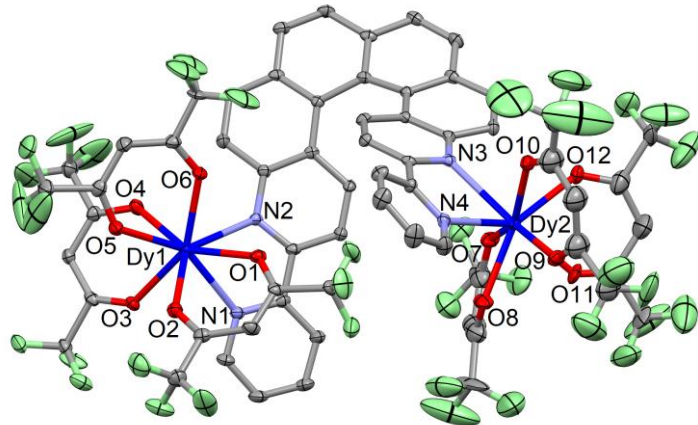


Figure S1. ORTEP view of **1**. Thermal ellipsoids are drawn at 30% probability. Hydrogen atoms and solvent molecules of crystallization are omitted for clarity.

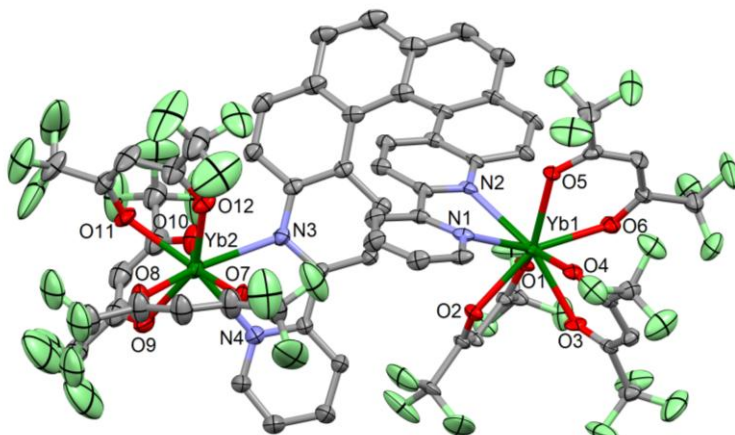


Figure S2. ORTEP view of **2**. Thermal ellipsoids are drawn at 30% probability. Hydrogen atoms and solvent molecules of crystallization are omitted for clarity.

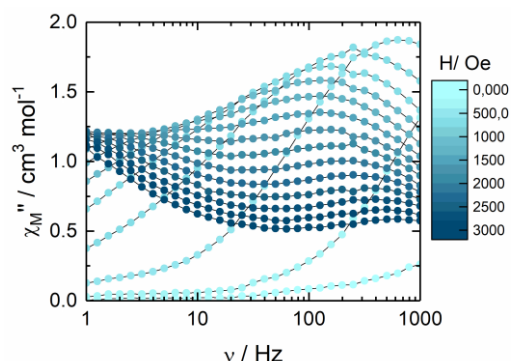


Figure S3. Field dependence of the out-of-phase component of the magnetic susceptibility for **1** at 2 K.

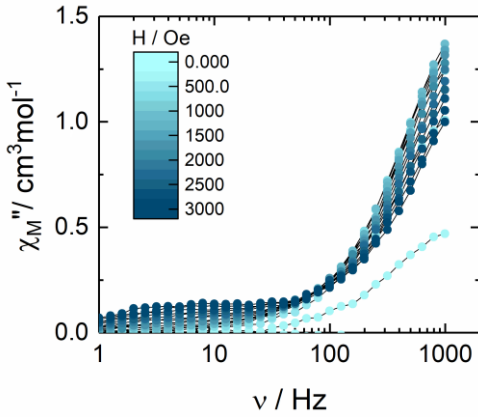


Figure S4. Field dependence of the out-of-phase component of the magnetic susceptibility for **2** at 2 K.

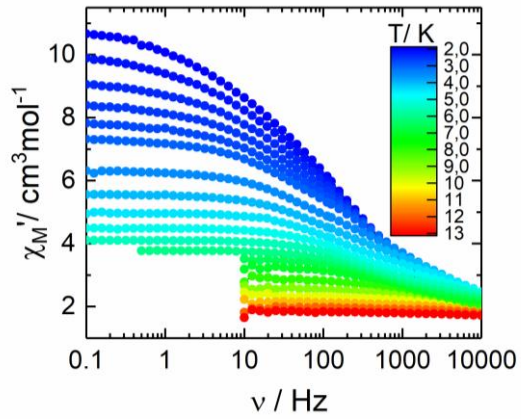


Figure S5. Frequency dependence of the in-phase component of the magnetic susceptibility for **1**.

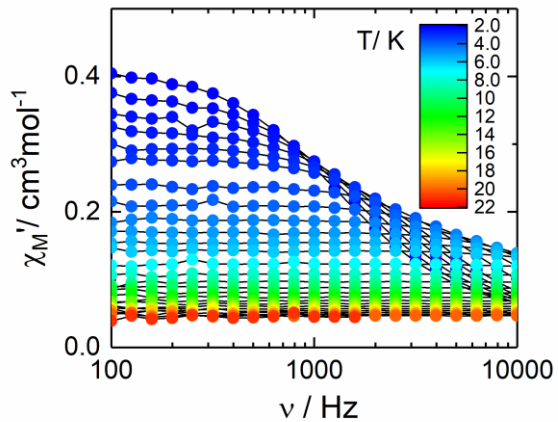


Figure S6. Frequency dependence of the in-phase component of the magnetic susceptibility for **2**.

Extended Debye model.

$$\chi_M' = \chi_s + (\chi_T - \chi_s) \frac{1 + (\omega\tau)^{1-\alpha} \sin\left(\alpha \frac{\pi}{2}\right)}{1 + 2(\omega\tau)^{1-\alpha} \sin\left(\alpha \frac{\pi}{2}\right) + (\omega\tau)^{2-2\alpha}}$$

$$\chi_M'' = (\chi_T - \chi_s) \frac{(\omega\tau)^{1-\alpha} \cos\left(\alpha \frac{\pi}{2}\right)}{1 + 2(\omega\tau)^{1-\alpha} \sin\left(\alpha \frac{\pi}{2}\right) + (\omega\tau)^{2-2\alpha}}$$

With χ_T the isothermal susceptibility, χ_s the adiabatic susceptibility, τ the relaxation time and α an empiric parameter which describe the distribution of the relaxation time. For SMM with only one relaxing object α is close to zero. The extended Debye model was applied to fit simultaneously the experimental variations of χ_M' and χ_M'' with the frequency f of the oscillating field ($\omega = 2\pi f$). Typically, only the temperatures for which a maximum on the χ'' vs. f curves, have been considered. The best fitted parameters τ , α , χ_T , χ_s are listed in Table S3 and S4 with the coefficient of determination R^2 .

Table S1. X-ray crystallographic data of **1** and **2**.

Compounds	1	2
Formula	C₆₄H₂₆Dy₂F₃₆N₄O₁₂	C₇₀H₄₀Yb₂F₃₆N₄O₁₂
M / g.mol ⁻¹	2051.89	2159.14
Crystal system	Triclinic	Triclinic
Space group	P-1 (N°2)	P-1 (N°2)
Cell parameters	a = 12.2629(16) Å b = 16.534(2) Å c = 18.118(3) Å α = 79.414(5) ° β = 77.667(5) ° γ = 87.190(5) °	a = 12.2906(17) Å b = 17.962(3) Å c = 18.439(3) Å α = 90.015(5) ° β = 99.337(5) ° γ = 100.196(5) °
Volume/Å ³	3527.4(8)	3951.7(10)
Z	2	2
T/K	150 (2)	150 (2)
2θ range /°	4.24 ≤ 2θ ≤ 55.20	5.85 ≤ 2θ ≤ 54.97
ρ_{calc} / g.cm ⁻³	1.932	1.815
μ / mm ⁻¹	2.261	2.498
Number of reflections	75302	136147
Independent reflections	15733	17903
$F_0^2 > 2\sigma(F_0)^2$	11594	14464
Number of variables	1027	1025
R _{int} , R ₁ , ωR_2	0.0758, 0.0672, 0.1585	0.0489, 0.1070, 0.2547

Table S2. SHAPE analysis for **1** and **2**.

	CShM _{SAPR-8} (square antiprism)	CShM _{BTPR-8} (biaugmented trigonal prism)	CShM _{TDD-8} (triangular dodecahedron)
	D _{4d}	C _{2v}	D _{2d}
	Dy1 1	2.616 1.480	2.626 1.677
	0.589		
	1.704		
	1.632		
	1.268		
		1.671 2.612	0.600 1.165

Table S3. Best-fitted parameters (χ_T , χ_S , τ and α) with the extended Debye model 2 at 1000 Oe field in the temperature range 2.0-4 K.

T/K	$\chi_T/\text{cm}^3 \text{ mol}^{-1}$	$\chi_S/\text{cm}^3 \text{ mol}^{-1}$	α	τ/s	R^2
2	0,41509	0,04357	0,12382	1,19997E-4	0,99975
2.2	0,37815	0,04077	0,11062	9,3418E-5	0,9996
2.4	0,34762	0,03734	0,10312	7,35554E-5	0,99897
2.6	0,32366	0,03498	0,10083	5,89835E-5	0,99934
2.8	0,29902	0,03472	0,08331	4,7948E-5	0,99948
3	0,28054	0,03121	0,08488	3,93158E-5	0,99954
3.5	0,23989	0,03147	0,05495	2,51774E-5	0,99925
4	0,21184	0,02786	0,05772	1,65059E-5	0,99941

Table S4. Computed energy levels (the ground state is set at zero), component values of the Lande factor g and wavefunction composition for each MJ state of the ground-state multiplet for Dy1 of **1**.

KD	Energy (cm ⁻¹)	g _x	g _y	g _z	Wavefunction composition *
1	0.0	1.34	2.01	14.94	0.30 ±13/2> + 0.27 ±11/2> + 0.23 ±15/2> + 0.11 ±7/2>
2	55.9	4.98	6.34	9.80	0.22 ±5/2> + 0.19 ±11/2> + 0.16 ±3/2> + 0.13 ±13/2> + 0.12 ±9/2>
3	143.9	4.20	5.04	9.49	0.29 ±13/2> + 0.27 ±9/2> + 0.10 ±3/2> + 0.10 ±1/2>
4	297.4	4.00	5.62	8.84	0.25 ±15/2> + 0.20 ±1/2> + 0.16 ±9/2> + 0.14 ±13/2> + 0.11 ±7/2>
5	383.5	1.39	3.91	13.17	0.30 ±7/2> + 0.18 ±5/2> + 0.13 ±11/2> + 0.11 ±3/2> + 0.10 ±1/2>
6	412.3	0.60	3.58	12.30	0.28 ±1/2> + 0.16 ±9/2> + 0.13 ±15/2> + 0.13 ±11/2> + 0.12 ±5/2>
7	510.8	0.80	3.37	12.45	0.25 ±3/2> + 0.23 ±15/2> + 0.16 ±11/2> + 0.14 ±9/2>
8	662.7	0.80	0.75	17.87	0.35 ±5/2> + 0.22 ±7/2> + 0.19 ±3/2> + 0.11 ±1/2>

* Only the contributions $\geq 10\%$ are given.

Table S5. Computed energy levels (the ground state is set at zero), component values of the Lande factor g and wavefunction composition for each MJ state of the ground-state multiplet for Dy2 of **1**.

KD	Energy (cm ⁻¹)	g _x	g _y	g _z	Wavefunction composition *
1	0.0	0.17	0.33	18.97	0.86 ±15/2> + 0.11 ±11/2>
2	96.0	0.83	1.45	15.46	0.54 ±13/2> + 0.29 ±9/2>
3	164.0	0.82	2.60	13.48	0.32 ±7/2> + 0.30 ±11/2> + 0.14 ±5/2>
4	204.6	0.08	0.74	17.35	0.21 ±11/2> + 0.20 ±1/2> + 0.14 ±5/2> + 0.14 ±3/2> + 0.13 ±13/2>
5	230.9	8.95	6.55	3.19	0.23 ±9/2> + 0.21 ±13/2> + 0.20 ±5/2> + 0.12 ±3/2>
6	273.5	2.48	3.22	13.56	0.25 ±1/2> + 0.23 ±3/2> + 0.17 ±7/2> + 0.12 ±11/2> + 0.10 ±9/2>
7	327.2	0.32	0.63	18.43	0.27 ±5/2> + 0.21 ±7/2> + 0.17 ±9/2> + 0.15 ±3/2> + 0.11 ±11/2>
8	652.7	0.01	0.01	19.76	0.43 ±1/2> + 0.31 ±3/2> + 0.16 ±5/2>

* Only the contributions $\geq 10\%$ are given.